Downloaded from jnm.snmjournals.org by on March 5, 2020. For personal use only.

Value of ^{18}F-FDG PET and PET/CT for Evaluation of Pediatric Malignancies

Lebriz Uslu[1], Jessica Donig[1], Michael Link[2], Jarrett Rosenberg[1], Andrew Quon[1], and Heike E. Daldrup-Link[1]

[1]*Department of Radiology, Molecular Imaging Program at Stanford, Stanford University, Stanford, California; and* [2]*Department of Pediatrics, Stanford University School of Medicine, Stanford, California*

Learning Objectives: On successful completion of this activity, participants should be able to (1) understand the current status of the role of ^{18}F-FDG PET and PET/CT for staging and treatment monitoring of pediatric malignancies; (2) discuss the limitations of ^{18}F-FDG PET and PET/CT for pediatric cancer imaging; and (3) discuss areas of pediatric cancer imaging in which further studies are needed.

Financial Disclosure: The authors acknowledge support from the Child Health Research Institute, Stanford University. Dr. Uslu was a resident at the Department of Nuclear Medicine at Istanbul University Cerrahpasa Medical Faculty, Istanbul, Turkey. She was supported as a visiting scholar by the Scientific and Technological Research Council of Turkey (TÜBİTAK). The authors of this article have indicated no other relevant relationships that could be perceived as a real or apparent conflict of interest.

CME Credit: SNMMI is accredited by the Accreditation Council for Continuing Medical Education (ACCME) to sponsor continuing education for physicians. SNMMI designates each *JNM* continuing education article for a maximum of 2.0 AMA PRA Category 1 Credits. Physicians should claim only credit commensurate with the extent of their participation in the activity. For CE credit, SAM, and other credit types, participants can access this activity through the SNMMI website (http://www.snmmilearningcenter.org) through February 2015.

Successful management of solid tumors in children requires imaging tests for accurate disease detection, characterization, and treatment monitoring. Technologic developments aim toward the creation of integrated imaging approaches that provide a comprehensive diagnosis with a single visit. These integrated diagnostic tests not only are convenient for young patients but also save direct and indirect health-care costs by streamlining procedures, minimizing hospitalizations, and minimizing lost school or work time for children and their parents. ^{18}F-FDG PET/CT is a highly sensitive and specific imaging modality for whole-body evaluation of pediatric malignancies. However, recent concerns about ionizing radiation exposure have led to a search for alternative imaging methods, such as whole-body MR imaging and PET/MR. As we develop new approaches for tumor staging, it is important to understand current benchmarks. This review article will synthesize the current literature on ^{18}F-FDG PET/CT for tumor staging in children, summarizing questions that have been solved and providing an outlook on unsolved avenues.

Key Words: pediatric oncology; positron emission tomography; PET/CT; pediatric cancer imaging; cancer staging; pediatric lymphoma; pediatric sarcoma

J Nucl Med 2015; 56:274–286
DOI: 10.2967/jnumed.114.146290

The use of ^{18}F-FDG PET and PET/CT imaging as a clinical tool for staging and restaging some but not all pediatric tumors has been established. Several studies have demonstrated improved sensitivities and specificities for ^{18}F-FDG PET/CT compared with all collective standard staging procedures, specifically for patients with lymphomas, sarcomas, and head and neck cancers (*1–4*). However, exposure of children to radiation through ^{18}F-FDG PET/CT is of concern to the pediatric imaging community (*5,6*), and various low-dose approaches are being pursued (*7–9*). A thorough understanding of the state of knowledge is needed to preserve the advantages of current ^{18}F-FDG PET/CT staging tests and create new imaging tests without compromises.

To this end, we performed a comprehensive MEDLINE literature search using the terms (child OR teen OR adolesc OR pediatric OR infant OR newborn OR neonat) AND ("Positron-Emission Tomography and Computed Tomography" OR "pet/ct" OR "Hybrid Pet and CT" OR "integrated pet ct" OR "SPECT and CT" OR "pet ct" OR "CT and PET"). This search identified 762 articles, which were further filtered regarding the following inclusion criteria: original research articles related to ^{18}F-FDG PET or ^{18}F-FDG PET/CT, pediatric or adolescent population only (up to age 23 y), malignant diseases, and minimum sample size of 10 cases per article. This led to 65 original research articles, which will be reviewed and summarized in this article, including 11 articles that were further evaluated with a metaanalysis. The metaanalysis provided information about the sensitivity, specificity, and accuracy of ^{18}F-FDG PET or ^{18}F-FDG PET/CT for staging and therapy response assessment of malignant lymphomas, with histopathology or clinical and imaging follow-up as the reference standard.

Although staging tests for pediatric cancers were originally performed with stand-alone ^{18}F-FDG PET scanners (*10–12*), these have been largely replaced by integrated ^{18}F-FDG PET/CT scanners (*13,14*). The added CT component improves the diagnostic accuracy of PET alone by adding a higher anatomic resolution to the acquired image information, thus improving lesion detection and characterization (*15*). Overall, the reported sensitivities of ^{18}F-FDG PET/CT for tumor staging in children are 90%–97% and the reported specificities are 99%–100% (*16–18*). These data refer to specific subsets of common pediatric malignancies, mainly

Received Aug. 25, 2014; revision accepted Dec. 2, 2014.
For correspondence contact either of the following:
Heike E. Daldrup-Link, Department of Radiology, Pediatric Radiology Section, Lucile Packard Children's Hospital, Stanford University, 725 Welch Rd., Stanford, CA 94304.
E-mail: heiked@stanford.edu
Andrew Quon, Division of Nuclear Medicine, Stanford University Medical Center, 300 Pasteur Dr., H2200, Stanford, CA 94305.
E-mail: aquon@stanford.edu
Published online Jan. 8, 2015.
COPYRIGHT © 2015 by the Society of Nuclear Medicine and Molecular Imaging, Inc.

Downloaded from jnm.snmjournals.org by on March 5, 2020. For personal use only.

lymphomas, sarcomas, and small cell neoplasms, and cannot be generalized to other pediatric malignancies. When the findings of different imaging tests were discrepant, ^{18}F-FDG PET/CT was found to be the accurate modality in 90% of evaluated cases (*16*). Importantly, the results of PET/CT scans demonstrated an impact on clinical decisions and patient management. For example, in a study on pediatric patients with lymphoma, Ewing sarcoma, primitive neuroectodermal tumor, or medulloblastoma, ^{18}F-FDG PET/CT changed the staging results in 61% of cases when compared with conventional imaging modalities (including CT, MR imaging, and ultrasonography) (*19*). Diagnostic information obtained from ^{18}F-FDG PET scans changed management in 24% of pediatric oncology patients, including those with lymphoma, sarcoma, central nervous system tumor, and plexiform neurofibroma (*20*). In this article, we will review how ^{18}F-FDG PET and PET/CT contributed to the staging and treatment monitoring of malignant tumors in pediatric patients.

MALIGNANT LYMPHOMA

Lymphoma is the third most common malignancy in the pediatric population (after leukemia and malignant brain tumors), comprising nearly 15% of childhood malignancies and 1,700 new diagnoses per year (53% Hodgkin lymphoma [HL] and 47% non-Hodgkin lymphoma [NHL]) (*21*). Classic HL accounts for more than 85% of cases of HL, whereas nodular lymphocyte-predominant HL is a less common subtype. NHL is a more heterogeneous group and includes high-grade lymphomas such as Burkitt lymphoma and Burkittlike tumors, which are more common in younger patients (5–14 y); diffuse large B-cell lymphomas, which are more common in older children and adolescents (15–19 y); and lymphoblastic lymphoma and anaplastic large cell lymphoma (1.4–13 y) (*22*). Rarer subtypes are also seen. Indolent lymphomas are uncommon in children (<5% of pediatric NHL), unlike adults (*23*). The 5-y survival rate is 95% for HL and 78% for NHL (*21,24*).

Initial Staging

Many studies have shown that ^{18}F-FDG PET or PET/CT is superior for staging malignant lymphomas when compared with conventional imaging modalities, including contrast-enhanced CT, MR imaging, bone scintigraphy, ultrasonography, and ^{67}Ga-scintigraphy (*11,12,14,25–27*). Most histologic subtypes of NHL in children are of high histologic grade and show strong ^{18}F-FDG uptake (*28,29*). Indolent lymphomas, such as extranodal marginal zone lymphoma, small lymphocytic lymphoma, and peripheral T-cell lymphoma, are rare in children. These subtypes generally show little or no ^{18}F-FDG uptake (*28,30*) or remain localized for long periods (*31*) and, thus, are usually not referred for ^{18}F-FDG PET/CT staging examinations (*32*).

The sensitivities and specificities of ^{18}F-FDG PET/CT or ^{18}F-FDG PET for initial staging of malignant lymphomas are 96%–99% and 95%–100%, respectively (Table 1) (*11,12,14,33,34*). ^{18}F-FDG PET is more sensitive than CT in detecting nodal and extranodal lesions in HL and NHL, including lesions in the spleen and bone marrow (Fig. 1) (*11,13*). CT, on the other hand, is more sensitive in the evaluation of pulmonary involvement: the positron range of ^{18}F-FDG limits the spatial resolution of PET, and continuous breathing during PET data acquisition impairs the detection of small pulmonary nodules (*11,13*). Although lung metastases are not common in HL, thoracic CT was reported to be more sensitive than ^{18}F-FDG PET in the detection of pulmonary lesions in HL patients (70% vs. 100%) (*11*). Detection of bone marrow involvement is important, as it upstages the patient to stage IV disease, which changes prognosis and management. Bone marrow biopsy is used for clinical staging decisions but obtains information from a limited area, typically the iliac crest. ^{18}F-FDG PET/CT provides information about the entire bone marrow, beyond clinical biopsy areas (Table 2) (*35–37*). Several authors reported that ^{18}F-FDG PET/CT accurately detected bone marrow involvement outside the pelvis in patients with negative results from routine biopsies of the iliac crest (*35–38*) and have suggested that ^{18}F-FDG PET/CT can supplant marrow biopsy for purposes of staging.

Therapy Response Assessment

Standard-of-care treatment of pediatric HL typically involves chemotherapy, which may be followed by involved-field radiotherapy in some patients. Patients with early-stage HL often do not receive radiotherapy, whereas those with intermediate and advanced stages have demonstrated improved progression-free survival with radiotherapy (*39*). Tumor response to chemotherapy is used as a criterion to determine the need for radiotherapy and the radiation dose. If radiotherapy is necessary, the radiation field is planned according to the initial extent of disease. Patients with NHL represent a heterogeneous group, which is typically treated with chemotherapy. The use of radiotherapy is limited in pediatric NHL (*40,41*).

Several investigators reported, for both pediatric HL and pediatric NHL, that additional information obtained on ^{18}F-FDG PET scans compared with CT scans changed management in up to 32% of patients (*20,42,43*). The most frequent management impact was avoiding radiotherapy of soft-tissue masses in HL, which did not show significant hypermetabolism on ^{18}F-FDG PET scans at the end of therapy. In 17% of advanced-stage HL, additional disease sites detected on ^{18}F-FDG PET/CT compared with CT alone resulted in an extended radiation field (*33*).

It is important to identify nonresponders early, to avoid ineffective treatments and enable early stratification to intensified or alternative treatment options. Likewise, correct identification of patients who could be spared from radiotherapy is important to avoid radiation-related complications. In both pediatric HL and pediatric NHL, the level of ^{18}F-FDG tumor uptake on interim ^{18}F-FDG PET/CT scans after initiation of chemotherapy has shown higher accuracy for therapy response assessment than evaluations of changes in tumor size on conventional imaging (*14,25,27,44*). However, interim ^{18}F-FDG PET/CT scans after 2–3 cycles of standard chemotherapy showed a relatively wide range of sensitivity (77.8%–100%) and specificity (54.5%–97.7%) (Table 1) (*26, 38,45,46*). This may be due to lack of consensus on the best timing of interim PET and the definition of objective response criteria for interpretation (*47–49*). Nevertheless, interim ^{18}F-FDG PET/CT has shown high negative predictive value, and therefore an early negative scan is a reliable indicator for therapy response (negative predictive value, 85.7%–100%; positive predictive value, 41.2%–85.7%) (*26,38,45*). In HL patients, Furth et al. reported that a negative interim ^{18}F-FDG PET/CT scan after 2 cycles of chemotherapy is a strong indicator of relapse-free survival, with a negative predictive value of 100% (*46*). Therefore, an interim ^{18}F-FDG PET/CT scan has been advocated by many investigators and has led to early intensification of chemotherapy in apparent nonresponders (*46,50,51*). A substantial fraction (≤65%) of patients with positive interim PET results will still be cured, and patients with negative or positive interim results seem to do well if their PET results are negative at the completion of chemotherapy (typically

Downloaded from jnm.snmjournals.org by on March 5, 2020. For personal use only.

TABLE 1
Diagnostic Value of ^{18}F-FDG PET and ^{18}F-FDG PET/CT for Staging and Restaging of Pediatric Patients with Malignant Lymphoma

Study	Type of disease	Device	Patients (*n*)	Design	Timing	Sensitivity	Specificity	PPV	NPV
Miller (*14*)	HL&NHL	PET/CT	31	Retrospective	Staging	99%	100%	100%	86%
Furth (*12*)	HL	PET	33	Prospective	Staging	84%	95%	87%	94%
Paulino (*33*)	HL	PET/CT	53	Retrospective	Staging	98.7%	97.6%	97.4%	98.8%
Punwani (*34*)	HL&NHL	PET/CT	29	Prospective	Staging	99.2%	100%	100%	99.8%
Kabickova (*11*)	HL	PET	55	Prospective	Staging	96.4%	100%	100%	71.4%
Furth (*46*)	HL	PET	40	Prospective	Interim (after 2 cycles chemotherapy)	100%	68.4%	14.3%	100%
Riad (*26*)	HL&NHL	PET/CT	152	Retrospective	Interim (after 2–3 cycles chemotherapy)	100%	97.7%	85.7%	100%
Bakhshi (*38*)	NHL	PET/CT	34	Prospective	Interim (after 2 cycles chemotherapy; 1.5–2 mo after therapy initiation)	77.8%	54.5%	41.2%	85.7%
Ilivitzki (*45*)	HL	PET/CT	34	Prospective	Interim (after 2 cycles chemotherapy)	85.7%	92.6%	75%	96.2%
Depas (*43*)	HL&NHL	PET	28	Retrospective	Interim (after 2–4 cycles chemotherapy or before chemo- or radiotherapy intensification)	NA	100%	NA	84.2%
Furth (*46*)	HL	PET	40	Prospective	Posttherapy (14–17 d after polychemotherapy end)	100%	78%	25%	100%
Levine (*50*)	HL	PET	47	Retrospective	Posttherapy	100%	84%	11%	100%
Meany (*51*)	HL	PET	23	Retrospective	Posttherapy	100%	57.1%	18.2%	100%
Bakhshi (*38*)	NHL	PET/CT	34	Prospective	Posttherapy (4–6 wk after chemotherapy end)	75%	75%	33.3%	95.7%
Riad (*26*)	HL&NHL	PET/CT	152	Retrospective	Posttherapy (3–8 wk after therapy end)	100%	90.9%	75%	100%
Depas (*43*)	HL&NHL	PET	28	Retrospective	Posttherapy (1–3 mo after therapy end)	NA	93.8%	NA	100%
Rhodes (*56*)	HL&NHL	PET/CT	41	Retrospective	Follow-up (median, 2.3 y)	95%	90%	53%	99.3%
Riad (*26*)	HL&NHL	PET/CT	152	Retrospective	Follow-up (mean, 6.8 mo)	100%	100%	100%	100%
Depas (*43*)	HL&NHL	PET	28	Retrospective	Follow-up (mean, 9 mo)	NA	94.9%	NA	100%
Hernandez-Pampaloni (*55*)	HL&NHL	PET	24	Retrospective	All	78%	98%	94%	80%
London (*27*)	HL&NHL	PET/CT	52	Retrospective	All	95.9%	99.7%	87.7%	99.9%
Lopci (*132*)	HL&NHL	PET	20	Prospective	All	100%	94%	89%	100%
Wickmann (*57*)	HL	PET	106	Retrospective	Staging and follow-up (2–26 wk after therapy end)	92.9%	55.6%	76.5%	83.3%

NA = data not available; NPV = negative predictive value; PPV = positive predictive value.

Downloaded from jnm.snmjournals.org by on March 5, 2020. For personal use only.

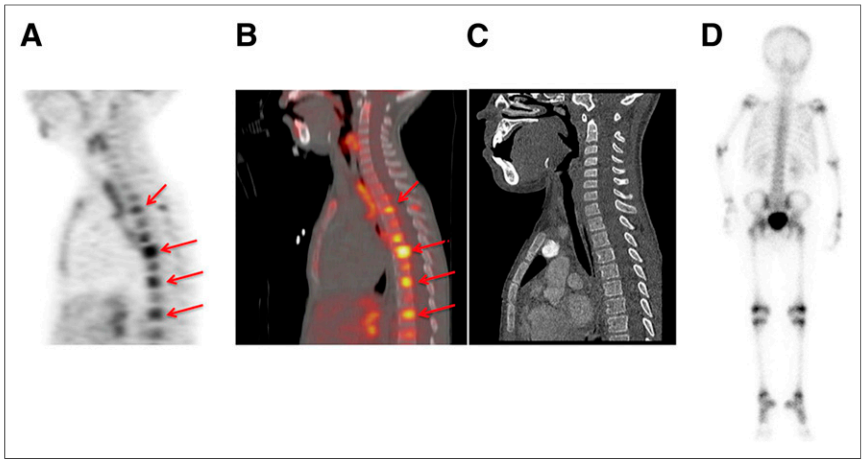


FIGURE 1. A 10-y-old girl with HL demonstrating multiple ^{18}F-FDG–avid bone metastases (arrows, A and B; SUV_{max}, 14.9) in thoracic spine that are not detectable on dedicated diagnostic CT (C) and radionuclide bone scanning (D).

6 cycles) (*52*). Therefore, other investigators suggest performing follow-up ^{18}F-FDG PET/CT scans at later time points (*53*).

In NHL patients, Yang et al. reported that a persistent tumor ^{18}F-FDG uptake on interim ^{18}F-FDG PET/CT scans predicted worse overall survival and event-free survival (*54*). However, this principle may not hold for all types of NHL (*38,43*). A recent study on nonlymphoblastic lymphoma patients showed that neither interim ^{18}F-FDG PET/CT nor interim CT scans could predict survival (*38*).

Reported sensitivities and specificities of ^{18}F-FDG PET/CT for therapy response assessment of HL and NHL at 2 wk to 3 mo after completion of therapy showed wide ranges of 75%–100% and 75%–90.9%, respectively (Table 1) (*26,38,46,50,51*). More systematic data evaluations are needed to determine the best time point for interim scans for response assessment of pediatric lymphomas.

Information about the value of ^{18}F-FDG PET or ^{18}F-FDG PET/CT follow-up studies of pediatric HL and NHL after therapy is based on few nonresponders per evaluated study population (*14,25, 43,46,50,55–57*). ^{18}F-FDG PET/CT has shown high sensitivity and specificity for the diagnosis of disease relapse in HL and NHL (95%–100% and 90%–100%, respectively) (Table 1) (*26,43,56*). However, false-positives were noted because of thymic rebound, inflamed lymph nodes, physiologic cardiac uptake (*43*), infections or inflammation (*56*), and reconverted marrow. This is a typical false-positive paradox, that is, false-positive results are more probable than true-positive when the overall population has a low incidence of a condition. Therefore, a negative follow-up ^{18}F-FDG PET scan is a strong indicator of absence of disease relapse, whereas a positive scan should be validated with other imaging modalities or biopsy (Fig. 2) (*56*).

Several recent studies have demonstrated that routine follow-up by ^{18}F-FDG PET/CT and other imaging techniques may be overused for routine surveillance of patients with HL, contributing to increased cost and radiation exposure without a clear survival benefit (*6,50,58*). More data are needed to determine which patient group will benefit from which surveillance test for how long and at which frequency. For example, Burkitt lymphoma nearly always recurs within the first year after treatment, whereas HL typically recurs within the first 2 y (*58–60*). Favorable prognostic indicators may allow limiting or omitting follow-up imaging. For example, patients with low-risk HL and negative ^{18}F-FDG PET results at the end of therapy do not require further imaging unless relapse is clinically suspected (*61–63*). Current guidelines for HL do not recommend routine follow-up ^{18}F-FDG PET scans for HL patients (*64,65*).

Tables 3 and 4 provide information about sensitivity, specificity, and accuracy of ^{18}F-FDG PET or PET/CT, as well as conventional imaging modalities, for staging or therapy response assessment of malignant lymphomas. The high degree of variability among these studies did not provide an adequate sample size for an inferential metaanalysis. However, the pooled data of 11 articles allowed an estimate of the per-modality accuracy (Fig. 3). Although the 95% confidence intervals for the 2 modalities overlap, the random-effects estimates of accuracy strongly suggest that PET is at least as accurate as, if not more accurate than, conventional imaging modalities (91% vs. 67%). Studies with large populations of pediatric patients are needed to confirm the additive value of PET.

TABLE 2
Diagnostic Value of ^{18}F-FDG PET and ^{18}F-FDG PET/CT for Detection of Bone Marrow Involvement in Pediatric Patients with Malignant Lymphoma

Study	Type of disease	Patients (*n*)	BMB sensitivity	BMB specificity	PET sensitivity in BM evaluation	PET specificity in BM evaluation
Agrawal (*35*)	HL	38	62.5%	100%	87.5%	100%
Cheng (*36*)	HL&NHL	54	54%	100%	92%	100%
Purz (*37*)	HL	175	NA	NA	100%	77.3%*, 92.2%†, 98.5%‡

*Confirmed only by positive BMB.
†Confirmed by BMB or multifocality.
‡Confirmed by BMB, multifocality, or chemotherapy response.
BM = bone marrow; BMB = bone marrow biopsy; NA = data not available.

Downloaded from jnm.snmjournals.org by on March 5, 2020. For personal use only.

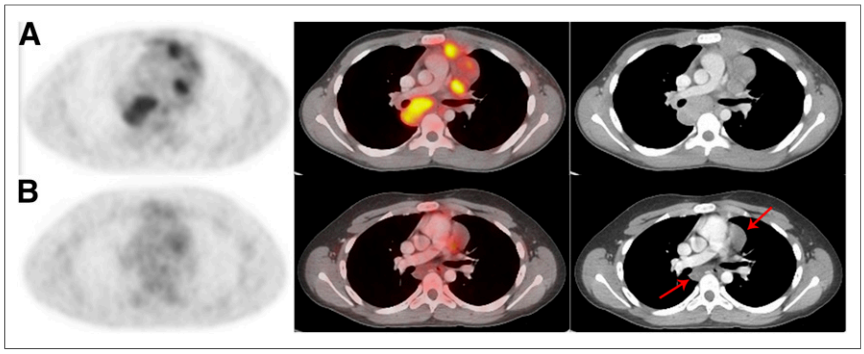


FIGURE 2. (A) A 14-y-old boy with multiple intensely ^{18}F-FDG–avid mediastinal lymph nodes on contrast-enhanced PET/CT consistent with HL at time of staging (SUV_{max}, 4.14). (B) Posttherapy contrast-enhanced ^{18}F-FDG PET/CT demonstrates persistent lymphadenopathy on CT (arrows). Lymphadenopathy is negative for ^{18}F-FDG activity, consistent with complete response to therapy. Patient achieved progression-free survival at 2 y follow-up.

BONE AND SOFT-TISSUE SARCOMAS

Bone and soft-tissue sarcomas account for 10% of all childhood malignancies and 8% of malignancies in adolescents and young adults (*66*), with an annual incidence of approximately 2 per 100,000 patients (*67*). The most common soft-tissue sarcomas in patients less than 20 y old are rhabdomyosarcomas (60% of soft-tissue sarcomas) (*1*, *68*), with an incidence of 4.5 cases per million per year (*68*). Fibrosarcomas, synovial sarcomas, and extraosseous Ewing sarcomas represent other soft-tissue sarcomas in the pediatric population (*69*). The most common bone sarcomas in children and adolescents are osteosarcomas and Ewing sarcoma family tumors, which comprise Ewing sarcoma of the bone, extraosseous Ewing sarcoma, primitive neuroectodermal tumors, neuroepithelioma, and Askin tumor (*70*).

Initial Staging

Most studies that evaluated ^{18}F-FDG PET/CT for staging of bone and soft-tissue sarcomas in children were based on small cohorts and heterogeneous collections of tumors (Table 5). The

TABLE 3
Characteristics of Studies Eligible for Metaanalysis

Study	Country	Data type	Study design	Device	Lymphoma subtype	Patients (*n*)	^{18}F-FDG dose (MBq/kg)	Gold standard
Agrawal (*35*)	India	Patients	Retrospective	PET/CT	HL	38	3.7	Follow-up and CT
Bakhshi (*38*)	India	Patients	Prospective	PET/CT	NHL	34	6–7	Follow-up imaging
Cheng (*36*)	USA	Patients	Retrospective	PET/CT	HL&NHL	54	5.18	Pathologic and clinical follow-up
Depas (*43*)	Belgium	Patients	Retrospective	PET	HL&NHL	28	3.7 or 2.2	Pathologic and clinical follow-up
Furth (*85*)	Germany	Patients	Prospective	PET	HL	40	NA	Pathologic, clinical, and imaging follow-up
Ilivitzki (*45*)	Israel	Patients	Prospective	PET/CT	HL	34	5.3	Follow-up ^{18}F-FDG PET
Lopci (*132*)	Italy	Patients	Prospective	PET	HL&NHL	20	5.3	Histopathologic and clinical follow-up
Meany (*51*)	USA	Patients	Retrospective	PET/CT?	HL	23	NA	Histopathologic, clinical, biochemical, and radiographic evaluation
Miller (*14*)	Israel	Patients	Retrospective	PET/CT	HL&NHL	31	7.4	Follow-up imaging
Purz (*37*)	Germany	Patients	Prospective	PET and PET/CT?	HL	175	NA	Bone marrow biopsy, MR imaging, CT, and clinical follow-up
Riad (*26*)	Egypt	Patients	Retrospective	PET/CT	HL&NHL	152	3.7	Pathologic and clinical follow-up

NA = data not available.

Downloaded from jnm.snmjournals.org by on March 5, 2020. For personal use only.

TABLE 4
Diagnostic Accuracy of ^{18}F-FDG PET and PET/CT in Studies Eligible for Metaanalysis

Study	True-positive	False-positive	True-negative	False-negative
Agrawal (*35*)	7	0	23	1
Bakhshi (*38*)	10	16	30	3
Cheng (*36*)	12	0	41	1
Depas (*43*)	18	4	47	4
Furth (*85*)	4	18	47	0
Ilivitzki (*45*)	6	2	25	1
Lopci (*132*)	14	2	25	0
Meany (*51*)	2	9	12	0
Miller (*14*)	3	0	19	1
Purz (*37*)	43	2	130	0
Riad (*26*)	20	4	87	0

presence of metastases is common in sarcomas and is associated with poor prognosis (*71,72*). Typical sites to be investigated with imaging tests are lymph nodes (more common in rhabdomyosarcomas, less common in bone sarcomas), lung, and bone (*73–75*). Nearly any other organ, such as brain, liver, and pancreas, can be affected as well (*73,76*). Tateishi et al. reported that in 16% of patients, ^{18}F-FDG PET/CT detected distant metastases that could not be detected with either conventional modalities or PET alone (*77*). The sensitivity and specificity of ^{18}F-FDG PET/CT for staging of all sarcomas ranged from 85.7%–100% and 97%–100%, respectively, for detection of nodal lesions to 56%–100% and 91%–100%, respectively, for detection of distant metastasis, including pulmonary lesions (Table 5) (*71,77–79*). For initial staging of rhabdomyosarcomas, the reported sensitivities and specificities of ^{18}F-FDG PET/CT were 93.8%–100% and 100%, respectively, for detection of nodal lesions and 100% and 91%, respectively, for detection of distant metastases (Fig. 4A) (*71,79*). In cases of bone sarcomas, ^{18}F-FDG PET/CT is more sensitive for the detection of extrapulmonary metastases (83.3% vs 77.8%) and more specific (98.1% vs. 96.7%) than conventional imaging modalities (*3*).

Pulmonary Metastases. Chest CT detected pulmonary metastases with higher sensitivity (93.3%–100%) than ^{18}F-FDG PET (25%) (*3,78*) because of the increased anatomic resolution of CT for detection of subcentimeter pulmonary nodules and variable ^{18}F-FDG uptake in pulmonary nodules (*2,3*).

^{18}F-FDG PET showed higher specificity in detecting malignant pulmonary nodules (95.8%) than did conventional imaging, including chest CT (87.3%) (Table 6) (*3*). Because the default clinical intervention for pulmonary nodules in sarcoma patients is surgical resection, it would be important to generate more reliable imaging indicators for exclusion of malignancy, which could avoid unnecessary surgeries of granulomas, intrapulmonary lymph nodes, and other benign lesions. Future studies should aim to ascertain specific imaging characteristics of benign lesions.

Bone Metastases. The detection of bone metastases significantly affects overall survival. For example, overall 3-y event-free survival in patients with metastatic rhabdomyosarcomas is 32% in the absence of bone metastases and only 15% in the presence of bone metastases (*80*).

Several studies on heterogeneous patient populations with bone and soft-tissue sarcomas demonstrated that in the detection of bone lesions, sensitivity and diagnostic accuracy were higher for ^{18}F-FDG PET/CT than for ^{99m}Tc-methylene diphosphonate bone scans (*81–84*) and conventional imaging (radiography, CT, MR imaging, and ultrasonography) (*78*). It was recommended that bone scans be omitted if bone sarcomas are evaluated with ^{18}F-FDG PET (*81*). The appropriateness of this recommendation was confirmed by studies that evaluated rhabdomyosarcomas and bone sarcomas separately: for detection of bone metastases in rhabdomyosarcomas, ^{18}F-FDG PET/CT showed a sensitivity of 100%, compared with 66% for conventional imaging modalities, including radiography, CT, MR imaging (*79*), or bone scintigraphy alone (*2,71*). For detection of bone metastases in Ewing sarcomas, ^{18}F-FDG PET showed a sensitivity of 88%, compared with 37% for conventional imaging modalities (*78*).

In osteosarcomas, however, the sensitivities of ^{18}F-FDG PET and conventional imaging modalities (radiography, CT, MR

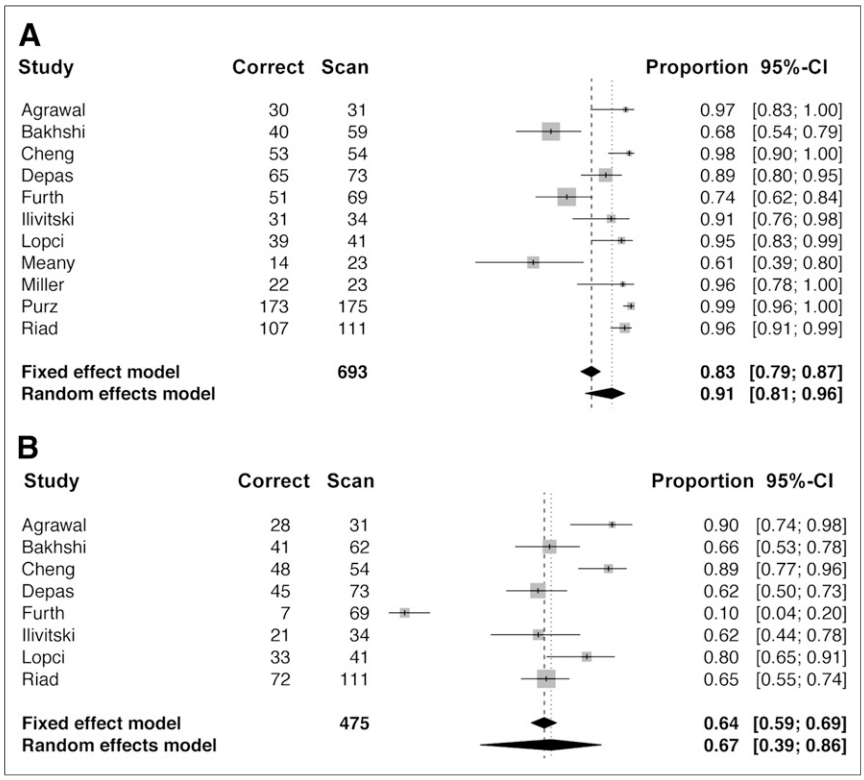


FIGURE 3. Overall diagnostic accuracy of ^{18}F-FDG PET or PET/CT (A) and conventional modalities (B) in pediatric lymphoma patients. Three studies reported only PET data.

Downloaded from jnm.snmjournals.org by on March 5, 2020. For personal use only.

TABLE 5
Diagnostic Value of ^{18}F-FDG PET and ^{18}F-FDG PET/CT for Staging and Restaging of Pediatric Patients with Malignant Sarcomas

Study	No. of disease cases	Patients (*n*)	Timing	Included lesions	Sensitivity	Specificity	PPV	NPV
Völker (*78*)	23 ESFT, 11 OS, 12 RMS	46	Initial staging	Nodal lesions	88%	97%	88%	97%
				Bone lesions	100%	91%	83%	100%
				Lung lesions	56%	100%	100%	90%
Tateishi (*77*)	20 ES, 18 OS, 5 SynS, 3 RMS, 1 FS, 1 EpS, 1 PleoMFH, 1 AS	50	Initial staging	Nodal lesions	85.71%	97.7%	85.7%	97.7%
				Distant metastases	70.8%	100%	100%	78.8%
Federico (*71*)	30 RMS	30	Initial staging	Nodal lesions	93.75%	100%	100%	95.24%
Eugene (*79*)	23 RMS	23	Initial staging	Nodal lesions	100%	100%	100%	100%
				Distant metastases	100%	91%	60%	100%
Arush (*95*)	9 ES, 3 OS, 7 RMS	19	Follow-up	Local recurrence	100%	92%	88%	100%
				Distant metastasis	77%	83%	91%	63%
London (*3*)	20 ES, 21 OS	41	All	All lesions	81.8%	97.5%	79.4%	97.8%
Mody (*133*)	16 ESFT, 9 RMS	25	All	All lesions	86%	80%	89%	67%
Walter (*81*)	12 ES, 9 OS, 8 STS	29	All	Bone lesions	100%	100%	100%	100%

PPV = positive predictive value; NPV = negative predictive value; ESFT = Ewing sarcoma family tumors; OS = osteosarcoma; RMS = rhabdomyosarcoma; ES = Ewing sarcoma; SynS = synovial sarcoma; FS = fibrosarcoma; EpS = epithelioid sarcoma; PleoMFH = pleomorphic malign fibrous histiocytoma; AS = angiosarcoma; STS = soft-tissue sarcoma.

imaging, and bone scintigraphy) for bone lesion detection were equal (90% for both) (*78*). The sensitivity of ^{18}F-FDG PET was only slightly higher than bone scintigraphy (90% vs. 81%), and this difference was not statistically significant (*78*). A likely explanation could be the higher osteoblastic activity in osteosarcoma metastases, as opposed to the predominant bone marrow infiltration in Ewing sarcomas (*78,83,85*).

Lymph Node Metastases. The presence of regional lymph node metastases is a strong prognostic factor in rhabdomyosarcoma patients (*72,86*). ^{18}F-FDG PET/CT was more sensitive (94%–100%) and more accurate (95%–100%) than conventional imaging (75%–94% and 49%–88%, respectively) for detection of lymph node metastases (*71,79*). Integrated ^{18}F-FDG PET/CT was also more accurate than ^{18}F-FDG PET alone (96% vs. 86%) (*77*). Ricard et al. reported that ^{18}F-FDG PET/CT changed lymph node staging in 4 of 13 rhabdomyosarcoma patients by downstaging 1 patient and detecting lymph node involvement not shown by conventional imaging modalities in 3 patients (*2*).

The low incidence of lymph node metastases in patients with osteosarcoma and Ewing sarcoma family tumors carries a risk of false-positive findings, since inflammatory lymph nodes with a high maximum standardized uptake value (SUV_{max}) are relatively more common. Thus, interventions are needed to decrease ^{18}F-FDG uptake by inflammatory nodes (and thereby decrease the incidence of false-positives), perhaps through antiinflammatory treatment before a staging ^{18}F-FDG PET/CT scan.

Prognostic Value. ^{18}F-FDG PET/CT can predict survival in pediatric sarcoma patients based on the metabolic activity of the primary tumor at the time of initial diagnosis (*1,87,88*). In a study on 41 rhabdomyosarcoma patients, hypermetabolism of the primary tumor ($SUV_{max}/SUV_{liver} > 4.6$) or metastases was linked to lower survival rates (*1*). In the same cohort, 44% of patients with high-intensity primary tumors (^{18}F-FDG uptake close to brain activity) at initial diagnosis died within 49 mo. By contrast, all patients with low-intensity primary tumors (^{18}F-FDG uptake $\leq$ liver activity) survived (*1*). Only 44% of patients with metabolically active lymph nodes and 50% of patients with hypermetabolic metastases survived (*1*).

Therapy Response Assessment

Neoadjuvant and adjuvant chemotherapy increased survival rates in sarcoma patients (*89–91*). Therapy response in clinical practice is currently assessed on the basis of change in the longest

Downloaded from jnm.snmjournals.org by on March 5, 2020. For personal use only.

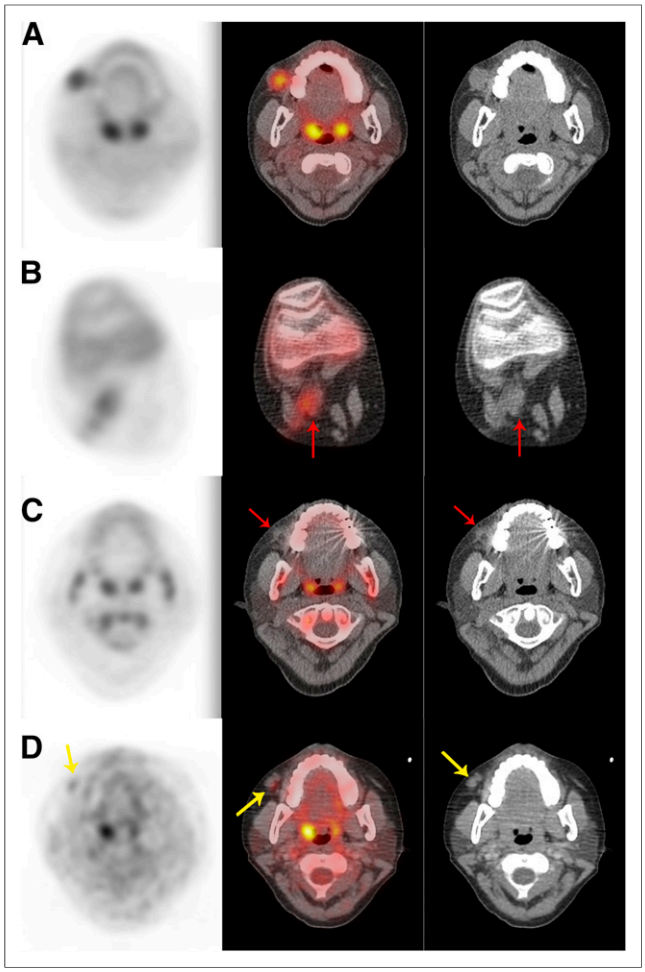


FIGURE 4. (A) An 11-y-old girl with ^{18}F-FDG–avid rhabdomyosarcoma identified on staging ^{18}F-FDG PET/CT in soft tissue overlying right maxilla, with SUV_{max} of 5.4. (B) Unexpected right popliteal lymph node metastasis discovered on staging whole-body ^{18}F-FDG PET/CT in transaxial plane (red arrow; SUV_{max}, 3.6). (C) Posttherapy ^{18}F-FDG PET/CT demonstrating resolution of ^{18}F-FDG activity in facial tumor (red arrows). (D) ^{18}F-FDG PET/CT showing new abnormal activity (yellow arrows; SUV_{max}, 2.2) consistent with recurrent tumor, confirmed by biopsy.

tumor diameter for soft-tissue sarcomas (Response Evaluation Criteria in Solid Tumors) and 3-dimensional changes in tumor size for bone sarcomas (Children's Oncology Group criteria). Metastases are evaluated by the same criteria if they are larger than 10 mm. A reduction in the soft-tissue component of bone sarcomas in response to chemotherapy does not necessarily predict a favorable outcome (*92*). Therefore, additional imaging biomarkers are needed to identify patients with poor outcomes and stratify these patients to more aggressive therapies.

There is some evidence that the degree of ^{18}F-FDG uptake on PET scanning may provide additional information for therapy response assessment, compared with morphologic assessments on CT and MR imaging scans (Table 7) (*92–94*).

In osteosarcomas, Denecke et al. reported that an overall tumor SUV and SUV_{max} on posttreatment ^{18}F-FDG PET/CT scans were more accurate for the assessment of therapy response than changes in tumor volume (*92*). Using a cutoff SUV_{max} of less than 2.8, ^{18}F-FDG PET/CT differentiated responders from nonresponders with up to 100% accuracy after completion of neoadjuvant therapy (*92, 93*). Im et al. even reported that an interim ^{18}F-FDG PET/CT scan after only a single course of neoadjuvant chemotherapy is useful in predicting tumor response (*94*). Histopathologic tumor response was associated with a median decrease of 75% in SUV_{max}, whereas nonresponders had a significantly lower decrease of 41% (*92*).

In Ewing sarcomas, ^{18}F-FDG PET/CT could not accurately predict therapy response, because both responders and nonresponders showed decreased ^{18}F-FDG tumor uptake (*92*). The predictive value of response on imaging tests is highly dependent on timing. In general, a patient who is responding well early after the initiation of therapy is likely to do well. As therapy continues, more patients will have responded and the test loses its predictive ability. For example, in acute lymphoblastic leukemia, 98% of patients will enter complete remission after 4 wk of chemotherapy, yet 20% will relapse. Thus, the assessment at 4 wk does not predict outcome very well (except for the 2% who do not reach any remission). Conversely, response assessment at 1 or 2 wk into therapy, when a smaller proportion of patients has attained remission, is more informative. Therefore, future studies should evaluate earlier ^{18}F-FDG PET assessments of response in Ewing sarcomas. In rhabdomyosarcomas, ^{18}F-FDG PET/CT correctly identified tumor response in 92% of patients after 3 cycles of chemotherapy, compared with 84% with conventional modalities (including chest radiography, bone marrow biopsy, contrast-enhanced CT, and contrast-enhanced MR imaging) (*79*).

Information about the value of ^{18}F-FDG PET/CT for the detection of tumor recurrence is limited. Arush et al. reported a high accuracy of ^{18}F-FDG PET/CT in the detection of local recurrence (95%) of Ewing sarcomas, osteosarcomas, and rhabdomyosarcomas

TABLE 6
Diagnostic Value of ^{18}F-FDG PET and ^{18}F-FDG PET/CT for Detection of Pulmonary Metastases in Pediatric Patients with Malignant Sarcomas

Study	Type of disease	Patients (*n*)	Timing of PET/CT	Sensitivity	Specificity	PPV	NPV
Völker (*78*)	OS, ES, RMS	46	Initial staging	25%	NA	100%	NA
London (*3*)	OS, ES	41	All	80.0%	95.8%	80%	95.8%
Cistaro (*134*)	OS, ES, ChS	18	Restaging	90.3%	93.8%	91.0%	93.3%

PPV = positive predictive value; NPV = negative predictive value; OS = osteosarcoma; ES = Ewing sarcoma; RMS = rhabdomyosarcoma; NA = data not available; ChS = chondrosarcoma.

Downloaded from jnm.snmjournals.org by on March 5, 2020. For personal use only.

TABLE 7
Assessment of Chemotherapy Response of Malignant Sarcomas in Pediatric Patients with ^{18}F-FDG PET/CT

Study	Type of disease	Patients (*n*)	Timing of PET/CT	Parameter	Sensitivity	Specificity	PPV	NPV
Im (*94*)	OS	20	Interim	SUV_{max}	100%	88.9%	83.3%	100%
				MTV	100%	88.9%	83.3%	100%
				TLG	100%	88.9%	83.3%	100%
			Therapy response	SUV_{max}	100%	88.9%	83.3%	100%
				MTV	60%	100%	100%	81.8%
				TLG	100%	77.8%	71.4%	100%
Denecke (*92*)	OS	27	Therapy response	Posttherapy SUV_{max}	80%	100%	100%	86%
				ΔSUV_{max}	100%	83%	83%	100%
				Visual interpretation	100%	100%	100%	100%
	ESFT		Therapy response	Posttherapy SUV_{max}	100%	50%	85%	100%
				ΔSUV_{max}	91%	50%	83%	67%
				Visual interpretation	100%	25%	79%	100%

PPV = positive predictive value; NPV = negative predictive value; OS = osteosarcoma; MTV = metabolic tumor volume; TLG = total lesion glycolysis; ESFT = Ewing sarcoma family tumor; ΔSUV_{max} = reduction in posttherapy SUV_{max} compared with pretherapy SUV_{max}.

on follow-up scans (Fig. 4B) (*95*). In the case of a new soft-tissue lesion on conventional imaging scans, which is of low suspicion for residual or recurrent disease, an ^{18}F-FDG PET/CT examination may be reassuring to exclude disease and avoid biopsy. In the case of any suggestive lesion, biopsy is warranted, and if the biopsy result is positive, ^{18}F-FDG PET/CT may be useful for restaging for additional tumor sites. More evidence is needed on diagnostic algorithms for the detection of tumor recurrence.

NEUROBLASTOMAS

Neuroblastoma is the most common pediatric extracranial soft-tissue tumor, accounting for 8% of all childhood malignancies (*96*). Its annual incidence is about 10.5 cases per 1 million children (*97*). Metastases to lymph nodes, liver, bone, and bone marrow are frequent in neuroblastoma patients, but nearly any other organ can be affected as well (*98*). ^{123}I- or ^{131}I-labeled metaiodobenzylguanidine (MIBG) is used as a biomarker for clinical whole-body staging and restaging with planar scintigraphy and SPECT (*96,99,100*). About 10% of neuroblastomas do not show MIBG uptake. In these patients, bone scans and ^{18}F-FDG PET scans were useful additional tools for whole-body staging (*96,99,101*).

Both MIBG-positive and MIBG-negative neuroblastomas demonstrated moderate ^{18}F-FDG uptake (Fig. 5) (*10,102*). The SUV_{max} of primary tumors was lower in early-stage (I–II) than advanced (III–IV) neuroblastoma (3.03 vs. 5.45, respectively, $P = 0.019$) (*103*). The inferior diagnostic accuracy of ^{18}F-FDG for the detection of distant metastases was mainly due to superior tumor-to-background contrast (*10*) and improved detection of bone and bone marrow disease with MIBG scintigraphy (*104*). The high metabolic activity of normal hematopoietic bone marrow in young children masked metastases on ^{18}F-FDG PET scans (*104*). Therefore, ^{123}I-MIBG scintigraphy was reported to be superior to ^{18}F-FDG PET in stage 4 neuroblastomas (*104*). Also, calvarial metastases in neuroblastoma patients may be masked by adjacent intense physiologic brain activity on ^{18}F-FDG PET scans (*105*). In another study, which primarily evaluated patients with advanced disease (no cranial vault lesions) after primary tumor resection and chemotherapy, MIBG scintigraphy and ^{18}F-FDG PET were equally effective in detecting bone metastases (*106*). This finding can be explained by the decreased metabolic activity of normal bone marrow after chemotherapy. However, other authors found that ^{18}F-FDG PET was problematic after granulocyte colony-stimulating factor therapy because of the associated increased bone marrow uptake (*104*).

Choi et al., in a study of 30 neuroblastoma patients, found that ^{18}F-FDG PET is more sensitive than CT in the evaluation of distant lymph node involvement and can help in detecting recurrent lymph node metastases (*103*). Therefore, ^{18}F-FDG PET/CT might be particularly helpful in older patients who present with small, resectable primary tumors and chronic lymph node metastases.

New radiotracers such as ^{124}I-MIBG PET (*107*), ^{18}F-DOPA (*108*), and ^{18}F-MIBG (*109*) may be the future for neuroblastoma staging and treatment monitoring. These tracers may obviate 24-h follow-up scans after tracer injection and enable theranostic approaches with combined diagnostic and therapeutic tracers.

WILMS TUMOR

Wilms tumor is the most common renal tumor in children, accounting for 6% of all pediatric malignancies and having an annual incidence of 500 cases in the United States. The overall 5-y survival rate exceeds 90% (*110*). Important information for local

Downloaded from jnm.snmjournals.org by on March 5, 2020. For personal use only.

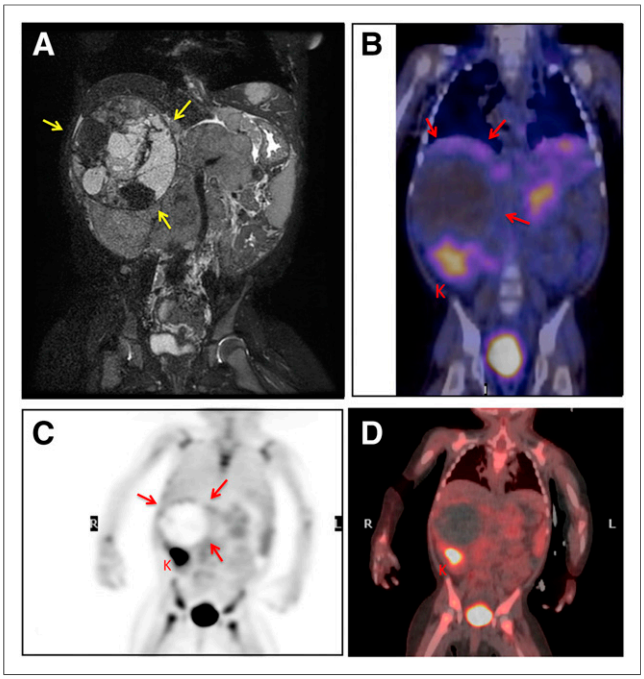


FIGURE 5. (A) A 2-y-old girl with large cystic abdominal neuroblastoma identified on coronal T2-weighted contrast MR imaging (yellow arrows) at time of diagnosis. (B–D) Pretherapy ^{123}I-MIBG-SPECT/CT (B), ^{18}F-FDG PET (C), and ^{18}F-FDG PET/CT (D) demonstrate subtle mild activity along rim of tumor (red arrows; SUV_{max}, 3.3). Patient had chemotherapy-related diffuse bone marrow activity. K = normal kidney.

tumor staging such as tumor location, size, local extension, vascular compression or invasion, and local lymph node metastases is best evaluated with CT, MR imaging, and ultrasonography (*111*). The most common site for metastases is the lungs, which are typically evaluated with chest CT (*111*). Therefore, ^{18}F-FDG PET is of limited value for assessment of Wilms tumors.

Wilms tumors show strong ^{18}F-FDG uptake (*112,113*), with a reported SUV_{mean} of 6.8 (*113*). Anaplastic Wilms tumors demonstrated particularly high ^{18}F-FDG uptake, with an SUV_{max} greater than 5, because of highly expressed glucose transporter 1 (*112*). There was otherwise no significant relation between ^{18}F-FDG uptake and tumor histopathology (*111*).

There are 2 major management approaches for Wilms tumor: one prefers initial surgery followed by chemotherapy, and the other prefers neoadjuvant chemotherapy followed by surgery (*114*). In patients who underwent preoperative systemic therapy, Misch et al. could not find any correlation between ^{18}F-FDG PET parameters (SUV reduction, initial SUV, posttherapy SUV, visual interpretation) and morphologic response assessments (volume reduction obtained by CT or MR imaging) (*113*). Conversely, Begent et al. reported lower tumor SUVs after chemotherapy in tumors that did respond to presurgical chemotherapy compared with those that did not (*112*). The differentiation between Wilms tumors and other kidney tumors would provide important information for patient management. To the best of our knowledge, no systematic studies exist that compare the degree and distribution of ^{18}F-FDG uptake in Wilms tumor, nephroblastomatosis, clear cell sarcoma, rhabdoid tumor, and renal cell carcinoma, among others. A study that could differentiate between Wilms tumor and nephroblastomatosis would be particularly clinically significant.

BRAIN TUMORS

Brain tumors are the most common solid tumors in children, accounting for 20%–25% of all childhood malignancies and having an annual incidence of nearly 2,200 cases (*115,116*). The most common brain tumors in pediatric patients are pilocytic astrocytomas (26.2% of childhood brain tumors) and primitive neuroectodermal tumors or medulloblastomas (21.9% of cases). Other types are gliomas (19.4%), ependymomas (7.8%), other astrocytomas (12.3%), glioblastomas (3.5%), oligodendrogliomas (1.9%), and others (0.7%) (*117*).

^{18}F-FDG PET/CT is not routinely used for clinical evaluation of pediatric brain tumors because the physiologic high ^{18}F-FDG uptake of the normal brain limits tumor detection, especially in low-grade gliomas (*118*). However, ^{18}F-FDG PET/CT may provide prognostic information based on the tumor's metabolic activity: in children with anaplastic astrocytomas, the degree of ^{18}F-FDG uptake was positively correlated with histopathologic tumor grade (*119*) and correlated with progression-free survival (*120*). In children with low-grade astrocytomas, progressive disease showed increased ^{18}F-FDG uptake, and initial hypermetabolism correlated with a shorter interval to progression (33 wk vs. 52.3 wk) (*121*). In children with brain stem gliomas, survival rates were significantly decreased when more than 50% of the tumor was ^{18}F-FDG–avid (*122*). Some benign tumors also demonstrate high ^{18}F-FDG uptake; these include juvenile pilocytic astrocytomas (*123*), choroid plexus papilloma (*124*), and pleomorphic xanthoastrocytoma (*125*), among others. More specific tracers that can better differentiate benign from malignant brain tumors, such as new amino acid tracers, choline analogs, or radiolabeled nucleoside analogs, are critically needed (*119*). Pirotte et al. suggested that absence of ^{18}F-FDG PET tumor uptake might justify more conservative treatment (*126*).

Evaluation of response to chemotherapy with ^{18}F-FDG PET is complicated in pediatric brain tumors because corticosteroids, chemotherapy, and radiation therapy all change cerebral glucose uptake (*127,128*). Interestingly, tumor metabolic activity, diagnosed with ^{18}F-FDG PET and MR spectroscopy, provide complementary information (*129*). The introduction of integrated PET/MR scanners may enable more detailed investigations of the clinical value of ^{18}F-FDG PET imaging in pediatric brain tumors. Non–^{18}F-FDG radiotracers such as 3′-deoxy-3′-^{18}F-fluorothymidine or ^{18}F-DOPA are promising tools for pediatric brain tumor imaging (*130,131*).

CONCLUSION

^{18}F-FDG PET/CT provides important information for staging and restaging of malignant lymphomas and other tumors in pediatric patients. However, the cumulative ionizing radiation dose caused by repeated ^{18}F-FDG PET/CT scans is a major concern for children. To address this issue, several guidelines have recently been developed for low-dose ^{18}F-FDG PET/CT protocols, involving injections of reduced radiotracer activity, low-dose CT protocols, and integration of CT scans for attenuation correction and diagnostic purposes.

For tumor staging of pediatric patients, recent developments in whole-body MR imaging and PET/MR provide alternatives with substantially reduced or even eliminated radiation exposure. Diagnostic accuracies, costs, and the clinical impact of these new technologies have to be tested against established PET/CT benchmarks. As we develop whole-body imaging technologies

Downloaded from jnm.snmjournals.org by on March 5, 2020. For personal use only.

further, it is important to not simply duplicate PET/CT approaches on different (and potentially more expensive) technologic pieces of equipment. We have to avoid reinventing the wheel by "discovering" advantages that have been previously identified on PET/CT studies. We hope that this article has helped to elucidate established concepts of PET and PET/CT technologies for pediatric cancer staging such that we can proceed to address unresolved questions, truly advancing this technology and making an impact on the lives of our patients.

REFERENCES

1. Baum SH, Fruhwald M, Rahbar K, Wessling J, Schober O, Weckesser M. Contribution of PET/CT to prediction of outcome in children and young adults with rhabdomyosarcoma. *J Nucl Med.* 2011;52:1535–1540.
2. Ricard F, Cimarelli S, Deshayes E, Mognetti T, Thiesse P, Giammarile F. Additional benefit of F-18 FDG PET/CT in the staging and follow-up of pediatric rhabdomyosarcoma. *Clin Nucl Med.* 2011;36:672–677.
3. London K, Stege C, Cross S, et al. ^{18}F-FDG PET/CT compared to conventional imaging modalities in pediatric primary bone tumors. *Pediatr Radiol.* 2012; 42:418–430.
4. Boktor RR, Omar WS, Mousa E, et al. A preliminary report on the impact of ^{18}F-FDG PET/CT in the management of paediatric head and neck cancer. *Nucl Med Commun.* 2012;33:21–28.
5. Chawla SC, Federman N, Zhang D, et al. Estimated cumulative radiation dose from PET/CT in children with malignancies: a 5-year retrospective review. *Pediatr Radiol.* 2010;40:681–686.
6. Nievelstein RA, Quarles van Ufford HM, Kwee TC, et al. Radiation exposure and mortality risk from CT and PET imaging of patients with malignant lymphoma. *Eur Radiol.* 2012;22:1946–1954.
7. Willowson KP, Bailey EA, Bailey DL. A retrospective evaluation of radiation dose associated with low dose FDG protocols in whole-body PET/CT. *Australas Phys Eng Sci Med.* 2012;35:49–53.
8. Alessio AM, Kinahan PE, Manchanda V, Ghioni V, Aldape L, Parisi MT. Weight-based, low-dose pediatric whole-body PET/CT protocols. *J Nucl Med.* 2009;50:1570–1577.
9. Klenk C, Gawande R, Uslu L, et al. Ionising radiation-free whole-body MRI versus ^{18}F-fluorodeoxyglucose PET/CT scans for children and young adults with cancer: a prospective, non-randomised, single-centre study. *Lancet Oncol.* 2014;15:275–285.
10. Shulkin BL, Mitchell DS, Ungar DR, et al. Neoplasms in a pediatric population: 2-[F-18]-fluoro-2-deoxy-D-glucose PET studies. *Radiology.* 1995;194:495–500.
11. Kabickova E, Sumerauer D, Cumlivska E, et al. Comparison of ^{18}F-FDG-PET and standard procedures for the pretreatment staging of children and adolescents with Hodgkin's disease. *Eur J Nucl Med Mol Imaging.* 2006;33:1025–1031.
12. Furth C, Denecke T, Steffen I, et al. Correlative imaging strategies implementing CT, MRI, and PET for staging of childhood Hodgkin disease. *J Pediatr Hematol Oncol.* 2006;28:501–512.
13. Cheng G, Servaes S, Zhuang H. Value of ^{18}F-fluoro-2-deoxy-D-glucose positron emission tomography/computed tomography scan versus diagnostic contrast computed tomography in initial staging of pediatric patients with lymphoma. *Leuk Lymphoma.* 2013;54:737–742.
14. Miller E, Metser U, Avrahami G, et al. Role of ^{18}F-FDG PET/CT in staging and follow-up of lymphoma in pediatric and young adult patients. *J Comput Assist Tomogr.* 2006;30:689–694.
15. Kleis M, Daldrup-Link H, Matthay K, et al. Diagnostic value of PET/CT for the staging and restaging of pediatric tumors. *Eur J Nucl Med Mol Imaging.* 2009;36:23–36.
16. Tatsumi M, Miller JH, Wahl RL. ^{18}F-FDG PET/CT in evaluating non-CNS pediatric malignancies. *J Nucl Med.* 2007;48:1923–1931.
17. Daldrup-Link HE, Franzius C, Link TM, et al. Whole-body MR imaging for detection of bone metastases in children and young adults: comparison with skeletal scintigraphy and FDG PET. *AJR.* 2001;177:229–236.
18. Kumar J, Seith A, Kumar A, et al. Whole-body MR imaging with the use of parallel imaging for detection of skeletal metastases in pediatric patients with small-cell neoplasms: comparison with skeletal scintigraphy and FDG PET/CT. *Pediatr Radiol.* 2008;38:953–962.
19. Odalović S, Sobic-Saranovic D, Pavlovic S, et al. Preliminary experience with 18f-fluoro-deoxy-glucose positron emission tomography/computed tomography in pediatric oncology patients. *Acta Chir Iugosl.* 2011;58:67–73.
20. Wegner EA, Barrington SF, Kingston JE, et al. The impact of PET scanning on management of paediatric oncology patients. *Eur J Nucl Med Mol Imaging.* 2005;32:23–30.
21. Percy CL, Smith MA, Linet M, Gloecker Ries LA, Friedman DL. Lymphomas and reticuloendothelial neoplasms. In: Ries LAG, Smith MA, Gurney JG, et al., eds. *Cancer Incidence and Survival Among Children and Adolescents: United States SEER Program 1975-1995.* Bethesda, MD: National Cancer Institute; 1999. NIH publication 99-4649.
22. Alessandri AJ, Pritchard SL, Schultz KR, Massing BG. A population-based study of pediatric anaplastic large cell lymphoma. *Cancer.* 2002;94:1830–1835.
23. Perkins SL, Gross TG. Pediatric indolent lymphoma: would less be better? *Pediatr Blood Cancer.* 2011;57:189–190.
24. Ward E, DeSantis C, Robbins A, Kohler B, Jemal A. Childhood and adolescent cancer statistics, 2014. *CA Cancer J Clin.* 2014;64:83–103.
25. Amthauer H, Furth C, Denecke T, et al. FDG-PET in 10 children with non-Hodgkin's lymphoma: initial experience in staging and follow-up. *Klin Padiatr.* 2005;217:327–333.
26. Riad R, Omar W, Kotb M, et al. Role of PET/CT in malignant pediatric lymphoma. *Eur J Nucl Med Mol Imaging.* 2010;37:319–329.
27. London K, Cross S, Onikul E, Dalla-Pozza L, Howman-Giles R. ^{18}F-FDG PET/CT in paediatric lymphoma: comparison with conventional imaging. *Eur J Nucl Med Mol Imaging.* 2011;38:274–284.
28. Weiler-Sagie M, Bushelev O, Epelbaum R, et al. ^{18}F-FDG avidity in lymphoma readdressed: a study of 766 patients. *J Nucl Med.* 2010;51:25–30.
29. Seam P, Juweid ME, Cheson BD. The role of FDG-PET scans in patients with lymphoma. *Blood.* 2007;110:3507–3516.
30. Elstrom R, Guan L, Baker G, et al. Utility of FDG-PET scanning in lymphoma by WHO classification. *Blood.* 2003;101:3875–3876.
31. Hoppe BS, Hodgson DC, Advani R, et al. ACR appropriateness criteria: localized nodal indolent lymphoma. *Oncology (Williston Park).* 2013;27:786–794.
32. Burton C, Ell P, Linch D. The role of PET imaging in lymphoma. *Br J Haematol.* 2004;126:772–784.
33. Paulino AC, Margolin J, Dreyer Z, Teh BS, Chiang S. Impact of PET-CT on involved field radiotherapy design for pediatric Hodgkin lymphoma. *Pediatr Blood Cancer.* 2012;58:860–864.
34. Punwani S, Taylor SA, Bainbridge A, et al. Pediatric and adolescent lymphoma: comparison of whole-body STIR half-Fourier RARE MR imaging with an enhanced PET/CT reference for initial staging. *Radiology.* 2010;255:182–190.
35. Agrawal K, Mittal BR, Bansal D, et al. Role of F-18 FDG PET/CT in assessing bone marrow involvement in pediatric Hodgkin's lymphoma. *Ann Nucl Med.* 2013;27:146–151.
36. Cheng G, Chen W, Chamroonrat W, Torigian DA, Zhuang H, Alavi A. Biopsy versus FDG PET/CT in the initial evaluation of bone marrow involvement in pediatric lymphoma patients. *Eur J Nucl Med Mol Imaging.* 2011;38:1469–1476.
37. Purz S, Mauz-Korholz C, Korholz D, et al. [^{18}F]fluorodeoxyglucose positron emission tomography for detection of bone marrow involvement in children and adolescents with Hodgkin's lymphoma. *J Clin Oncol.* 2011;29:3523–3528.
38. Bakhshi S, Radhakrishnan V, Sharma P, et al. Pediatric nonlymphoblastic non-Hodgkin lymphoma: baseline, interim, and posttreatment PET/CT versus contrast-enhanced CT for evaluation—a prospective study. *Radiology.* 2012;262: 956–968.
39. Dörffel W, Ruhl U, Luders H, et al. Treatment of children and adolescents with Hodgkin lymphoma without radiotherapy for patients in complete remission after chemotherapy: final results of the multinational trial GPOH-HD95. *J Clin Oncol.* 2013;31:1562–1568.
40. Link MP, Shuster JJ, Donaldson SS, Berard CW, Murphy SB. Treatment of children and young adults with early-stage non-Hodgkin's lymphoma. *N Engl J Med.* 1997;337:1259–1266.
41. Burkhardt B, Woessmann W, Zimmermann M, et al. Impact of cranial radiotherapy on central nervous system prophylaxis in children and adolescents with central nervous system-negative stage III or IV lymphoblastic lymphoma. *J Clin Oncol.* 2006;24:491–499.
42. Montravers F, McNamara D, Landman-Parker J, et al. [^{18}F]FDG in childhood lymphoma: clinical utility and impact on management. *Eur J Nucl Med Mol Imaging.* 2002;29:1155–1165.
43. Depas G, De Barsy C, Jerusalem G, et al. ^{18}F-FDG PET in children with lymphomas. *Eur J Nucl Med Mol Imaging.* 2005;32:31–38.
44. Mody RJ, Bui C, Hutchinson RJ, Frey KA, Shulkin BL. Comparison of ^{18}F flurodeoxyglucose PET with Ga-67 scintigraphy and conventional imaging modalities in pediatric lymphoma. *Leuk Lymphoma.* 2007;48:699–707.
45. Ilivitzki A, Radan L, Ben-Arush M, Israel O, Ben-Barak A. Early interim FDG PET/CT prediction of treatment response and prognosis in pediatric Hodgkin disease: added value of low-dose CT. *Pediatr Radiol.* 2013;43:86–92.

Downloaded from jnm.snmjournals.org by on March 5, 2020. For personal use only.

46. Furth C, Steffen IG, Amthauer H, et al. Early and late therapy response assessment with [^{18}F]fluorodeoxyglucose positron emission tomography in pediatric Hodgkin's lymphoma: analysis of a prospective multicenter trial. *J Clin Oncol.* 2009;27:4385–4391.
47. Le Roux PY, Gastinne T, Le Gouill S, et al. Prognostic value of interim FDG PET/CT in Hodgkin's lymphoma patients treated with interim response-adapted strategy: comparison of International Harmonization Project (IHP), Gallamini and London criteria. *Eur J Nucl Med Mol Imaging.* 2011;38:1064–1071.
48. Furth C, Erdrich AS, Steffen IG, et al. Interim PET response criteria in paediatric non-Hodgkin's lymphoma: results from a retrospective multicenter reading. *Nuklearmedizin.* 2013;52:148–156.
49. Furth C, Steffen IG, Erdrich AS, et al. Explorative analyses on the value of interim PET for prediction of response in pediatric and adolescent non-Hodgkin lymphoma patients. *EJNMMI Res.* 2013;3:71.
50. Levine JM, Weiner M, Kelly KM. Routine use of PET scans after completion of therapy in pediatric Hodgkin disease results in a high false positive rate. *J Pediatr Hematol Oncol.* 2006;28:711–714.
51. Meany HJ, Gidvani VK, Minniti CP. Utility of PET scans to predict disease relapse in pediatric patients with Hodgkin lymphoma. *Pediatr Blood Cancer.* 2007;48:399–402.
52. Sher DJ, Mauch PM, Van Den Abbeele A, LaCasce AS, Czerminski J, Ng AK. Prognostic significance of mid- and post-ABVD PET imaging in Hodgkin's lymphoma: the importance of involved-field radiotherapy. *Ann Oncol.* 2009;20:1848–1853.
53. Longo DL. Treatment of advanced Hodgkin lymphoma: the more things change, the more they stay the same. *J Clin Oncol.* 2013;31:660–662.
54. Yang DH, Min JJ, Jeong YY, et al. The combined evaluation of interim contrast-enhanced computerized tomography (CT) and FDG-PET/CT predicts the clinical outcomes and may impact on the therapeutic plans in patients with aggressive non-Hodgkin's lymphoma. *Ann Hematol.* 2009;88:425–432.
55. Hernandez-Pampaloni M, Takalkar A, Yu JQ, Zhuang H, Alavi A. F-18 FDG-PET imaging and correlation with CT in staging and follow-up of pediatric lymphomas. *Pediatr Radiol.* 2006;36:524–531.
56. Rhodes MM, Delbeke D, Whitlock JA, et al. Utility of FDG-PET/CT in follow-up of children treated for Hodgkin and non-Hodgkin lymphoma. *J Pediatr Hematol Oncol.* 2006;28:300–306.
57. Wickmann L, Luders H, Dorffel W. 18-FDG-PET-findings in children and adolescents with Hodgkin's disease: retrospective evaluation of the correlation to other imaging procedures in initial staging and to the predictive value of follow up examinations [in German]. *Klin Padiatr.* 2003;215:146–150.
58. Rathore N, Eissa HM, Margolin JF, et al. Pediatric Hodgkin lymphoma: are we over-scanning our patients? *Pediatr Hematol Oncol.* 2012;29:415–423.
59. Molyneux EM, Rochford R, Griffin B, et al. Burkitt's lymphoma. *Lancet.* 2012;379:1234–1244.
60. Friedmann AM, Wolfson JA, Hudson MM, et al. Relapse after treatment of pediatric Hodgkin lymphoma: outcome and role of surveillance after end of therapy. *Pediatr Blood Cancer.* 2013;60:1458–1463.
61. Voss SD. Pediatric oncology and the future of oncological imaging. *Pediatr Radiol.* 2011;41(suppl 1):S172–S185.
62. Voss SD. Surveillance imaging in pediatric Hodgkin lymphoma. *Curr Hematol Malig Rep.* 2013;8:218–225.
63. Voss SD, Chen L, Constine LS, et al. Surveillance computed tomography imaging and detection of relapse in intermediate- and advanced-stage pediatric Hodgkin's lymphoma: a report from the Children's Oncology Group. *J Clin Oncol.* 2012;30:2635–2640.
64. Follows GA, Ardeshna KM, Barrington SF, et al. Guidelines for the first line management of classical Hodgkin lymphoma. *Br J Haematol.* 2014;166:34–49.
65. Engert A, Eichenauer DA, Dreyling M. Hodgkin's lymphoma: ESMO Clinical Practice Guidelines for diagnosis, treatment and follow-up. *Ann Oncol.* 2010;21 (suppl 5):v168–v171.
66. Amankwah EK, Conley AP, Reed DR. Epidemiology and therapies for metastatic sarcoma. *Clin Epidemiol.* 2013;5:147–162.
67. Ducimetière F, Lurkin A, Ranchere-Vince D, et al. Incidence of sarcoma histotypes and molecular subtypes in a prospective epidemiological study with central pathology review and molecular testing. *PLoS ONE.* 2011;6:e20294.
68. Ognjanovic S, Linabery AM, Charbonneau B, Ross JA. Trends in childhood rhabdomyosarcoma incidence and survival in the United States, 1975-2005. *Cancer.* 2009;115:4218–4226.
69. Arndt CA, Crist WM. Common musculoskeletal tumors of childhood and adolescence. *N Engl J Med.* 1999;341:342–352.
70. Burns DK, Kumar V. The musculoskeletal system. In: Kumar V, Cotran RS, Robbins SL, eds. *Robbins Basic Pathology.* 7th ed. Philadelphia, Pennsylvania: Saunders; 2003:769–770.
71. Federico SM, Spunt SL, Krasin MJ, et al. Comparison of PET-CT and conventional imaging in staging pediatric rhabdomyosarcoma. *Pediatr Blood Cancer.* 2013;60:1128–1134.
72. Wharam MD, Meza J, Anderson J, et al. Failure pattern and factors predictive of local failure in rhabdomyosarcoma: a report of group III patients on the third Intergroup Rhabdomyosarcoma Study. *J Clin Oncol.* 2004;22:1902–1908.
73. Cormier JN, Pollock RE. Soft tissue sarcomas. *CA Cancer J Clin.* 2004;54:94–109.
74. Vincenzi B, Frezza AM, Schiavon G, et al. Bone metastases in soft tissue sarcoma: a survey of natural history, prognostic value and treatment options. *Clin Sarcoma Res.* 2013;3:6.
75. Billingsley KG, Burt ME, Jara E, et al. Pulmonary metastases from soft tissue sarcoma: analysis of patterns of diseases and postmetastasis survival. *Ann Surg.* 1999;229:602–610.
76. Ryzewicz M, McLoughlin HA, Freudenberger C, Williams A, Lindeque B. Unusual metastases from extremity soft tissue sarcomas. *Orthopedics.* 2008; 31:439.
77. Tateishi U, Hosono A, Makimoto A, et al. Accuracy of ^{18}F fluorodeoxyglucose positron emission tomography/computed tomography in staging of pediatric sarcomas. *J Pediatr Hematol Oncol.* 2007;29:608–612.
78. Völker T, Denecke T, Steffen I, et al. Positron emission tomography for staging of pediatric sarcoma patients: results of a prospective multicenter trial. *J Clin Oncol.* 2007;25:5435–5441.
79. Eugene T, Corradini N, Carlier T, Dupas B, Leux C, Bodet-Milin C. ^{18}F-FDG-PET/CT in initial staging and assessment of early response to chemotherapy of pediatric rhabdomyosarcomas. *Nucl Med Commun.* 2012;33:1089–1095.
80. Oberlin O, Rey A, Lyden E, et al. Prognostic factors in metastatic rhabdomyosarcomas: results of a pooled analysis from United States and European cooperative groups. *J Clin Oncol.* 2008;26:2384–2389.
81. Walter F, Czernin J, Hall T, et al. Is there a need for dedicated bone imaging in addition to ^{18}F-FDG PET/CT imaging in pediatric sarcoma patients? *J Pediatr Hematol Oncol.* 2012;34:131–136.
82. Franzius C, Sciuk J, Brinkschmidt C, Jurgens H, Schober O. Evaluation of chemotherapy response in primary bone tumors with F-18 FDG positron emission tomography compared with histologically assessed tumor necrosis. *Clin Nucl Med.* 2000;25:874–881.
83. Franzius C, Sciuk J, Daldrup-Link HE, Jurgens H, Schober O. FDG-PET for detection of osseous metastases from malignant primary bone tumours: comparison with bone scintigraphy. *Eur J Nucl Med.* 2000;27:1305–1311.
84. Györke T, Zajic T, Lange A, et al. Impact of FDG PET for staging of Ewing sarcomas and primitive neuroectodermal tumours. *Nucl Med Commun.* 2006; 27:17–24.
85. Furth C, Amthauer H, Denecke T, Ruf J, Henze G, Gutberlet M. Impact of whole-body MRI and FDG-PET on staging and assessment of therapy response in a patient with Ewing sarcoma. *Pediatr Blood Cancer.* 2006;47:607–611.
86. Mandell L, Ghavimi F, LaQuaglia M, Exelby P. Prognostic significance of regional lymph node involvement in childhood extremity rhabdomyosarcoma. *Med Pediatr Oncol.* 1990;18:466–471.
87. Franzius C, Bielack S, Flege S, Sciuk J, Jurgens H, Schober O. Prognostic significance of ^{18}F-FDG and ^{99m}Tc-methylene diphosphonate uptake in primary osteosarcoma. *J Nucl Med.* 2002;43:1012–1017.
88. Brenner W, Conrad EU, Eary JF. FDG PET imaging for grading and prediction of outcome in chondrosarcoma patients. *Eur J Nucl Med Mol Imaging.* 2004;31:189–195.
89. Marulanda GA, Henderson ER, Johnson DA, Letson GD, Cheong D. Orthopedic surgery options for the treatment of primary osteosarcoma. *Cancer Control.* 2008;15:13–20.
90. Arndt CA, Rose PS, Folpe AL, Laack NN. Common musculoskeletal tumors of childhood and adolescence. *Mayo Clin Proc.* 2012;87:475–487.
91. Bacci G, Longhi A, Fagioli F, Briccoli A, Versari M, Picci P. Adjuvant and neoadjuvant chemotherapy for osteosarcoma of the extremities: 27 year experience at Rizzoli Institute, Italy. *Eur J Cancer.* 2005;41:2836–2845.
92. Denecke T, Hundsdorfer P, Misch D, et al. Assessment of histological response of paediatric bone sarcomas using FDG PET in comparison to morphological volume measurement and standardized MRI parameters. *Eur J Nucl Med Mol Imaging.* 2010;37:1842–1853.
93. Hawkins DS, Rajendran JG, Conrad EU III, Bruckner JD, Eary JF. Evaluation of chemotherapy response in pediatric bone sarcomas by [F-18]-fluorodeoxy-D-glucose positron emission tomography. *Cancer.* 2002;94:3277–3284.
94. Im HJ, Kim TS, Park SY, et al. Prediction of tumour necrosis fractions using metabolic and volumetric ^{18}F-FDG PET/CT indices, after one course and at the completion of neoadjuvant chemotherapy, in children and young adults with osteosarcoma. *Eur J Nucl Med Mol Imaging.* 2012;39:39–49.
95. Arush MW, Israel O, Postovsky S, et al. Positron emission tomography/computed tomography with 18fluoro-deoxyglucose in the detection of local recurrence and distant metastases of pediatric sarcoma. *Pediatr Blood Cancer.* 2007;49: 901–905.

Downloaded from jnm.snmjournals.org by on March 5, 2020. For personal use only.

96. Sharp SE, Gelfand MJ, Shulkin BL. Pediatrics: diagnosis of neuroblastoma. *Semin Nucl Med.* 2011;41:345–353.
97. London WB, Castleberry RP, Matthay KK, et al. Evidence for an age cutoff greater than 365 days for neuroblastoma risk group stratification in the Children's Oncology Group. *J Clin Oncol.* 2005;23:6459–6465.
98. DuBois SG, Kalika Y, Lukens JN, et al. Metastatic sites in stage IV and IVS neuroblastoma correlate with age, tumor biology, and survival. *J Pediatr Hematol Oncol.* 1999;21:181–189.
99. Piccardo A, Lopci E, Conte M, et al. PET/CT imaging in neuroblastoma. *Q J Nucl Med Mol Imaging.* 2013;57:29–39.
100. Brodeur GM, Pritchard J, Berthold F, et al. Revisions of the international criteria for neuroblastoma diagnosis, staging, and response to treatment. *J Clin Oncol.* 1993;11:1466–1477.
101. Mueller WP, Coppenrath E, Pfluger T. Nuclear medicine and multimodality imaging of pediatric neuroblastoma. *Pediatr Radiol.* 2013;43:418–427.
102. Chawla M, Kumar R, Agarwala S, Bakhshi S, Gupta DK, Malhotra A. Role of positron emission tomography-computed tomography in staging and early chemotherapy response evaluation in children with neuroblastoma. *Indian J Nucl Med.* 2010;25:147–155.
103. Choi YJ, Hwang HS, Kim HJ, et al. ^{18}F-FDG PET as a single imaging modality in pediatric neuroblastoma: comparison with abdomen CT and bone scintigraphy. *Ann Nucl Med.* 2014;28:301–313.
104. Sharp SE, Shulkin BL, Gelfand MJ, Salisbury S, Furman WL. ^{123}I-MIBG scintigraphy and ^{18}F-FDG PET in neuroblastoma. *J Nucl Med.* 2009;50:1237–1243.
105. Papathanasiou ND, Gaze MN, Sullivan K, et al. ^{18}F-FDG PET/CT and ^{123}I-metaiodobenzylguanidine imaging in high-risk neuroblastoma: diagnostic comparison and survival analysis. *J Nucl Med.* 2011;52:519–525.
106. Kushner BH, Yeung HW, Larson SM, Kramer K, Cheung NK. Extending positron emission tomography scan utility to high-risk neuroblastoma: fluorine-18 fluorodeoxyglucose positron emission tomography as sole imaging modality in follow-up of patients. *J Clin Oncol.* 2001;19:3397–3405.
107. Vaidyanathan G, Affleck DJ, Zalutsky MR. Validation of 4-[fluorine-18]fluoro-3-iodobenzylguanidine as a positron-emitting analog of MIBG. *J Nucl Med.* 1995;36:644–650.
108. Lopci E, Piccardo A, Nanni C, et al. ^{18}F-DOPA PET/CT in neuroblastoma: comparison of conventional imaging with CT/MR. *Clin Nucl Med.* 2012;37:e73–e78.
109. Zhang H, Huang R, Pillarsetty N, et al. Synthesis and evaluation of ^{18}F-labeled benzylguanidine analogs for targeting the human norepinephrine transporter. *Eur J Nucl Med Mol Imaging.* 2014;41:322–332.
110. Smith MA, Seibel NL, Altekruse SF, et al. Outcomes for children and adolescents with cancer: challenges for the twenty-first century. *J Clin Oncol.* 2010;28:2625–2634.
111. Moinul Hossain AK, Shulkin BL, Gelfand MJ, et al. FDG positron emission tomography/computed tomography studies of Wilms' tumor. *Eur J Nucl Med Mol Imaging.* 2010;37:1300–1308.
112. Begent J, Sebire NJ, Levitt G, et al. Pilot study of F(18)-fluorodeoxyglucose positron emission tomography/computerised tomography in Wilms' tumour: correlation with conventional imaging, pathology and immunohistochemistry. *Eur J Cancer.* 2011;47:389–396.
113. Misch D, Steffen IG, Schonberger S, et al. Use of positron emission tomography for staging, preoperative response assessment and posttherapeutic evaluation in children with Wilms tumour. *Eur J Nucl Med Mol Imaging.* 2008;35:1642–1650.
114. Gleason JM, Lorenzo AJ, Bowlin PR, Koyle MA. Innovations in the management of Wilms' tumor. *Ther Adv Urol.* 2014;6:165–176.
115. Baldwin RT, Preston-Martin S. Epidemiology of brain tumors in childhood: a review. *Toxicol Appl Pharmacol.* 2004;199:118–131.
116. Pollack IF, Jakacki RI. Childhood brain tumors: epidemiology, current management and future directions. *Nat Rev Neurol.* 2011;7:495–506.
117. McKean-Cowdin R, Razavi P, Barrington-Trimis J, et al. Trends in childhood brain tumor incidence, 1973-2009. *J Neurooncol.* 2013;115:153–160.
118. Kim S, Salamon N, Jackson HA, Bluml S, Panigrahy A. PET imaging in pediatric neuroradiology: current and future applications. *Pediatr Radiol.* 2010;40:82–96.
119. Borgwardt L, Hojgaard L, Carstensen H, et al. Increased fluorine-18 2-fluoro-2-deoxy-D-glucose (FDG) uptake in childhood CNS tumors is correlated with malignancy grade: a study with FDG positron emission tomography/magnetic resonance imaging coregistration and image fusion. *J Clin Oncol.* 2005;23:3030–3037.
120. Williams G, Fahey FH, Treves ST, et al. Exploratory evaluation of two-dimensional and three-dimensional methods of FDG PET quantification in pediatric anaplastic astrocytoma: a report from the Pediatric Brain Tumor Consortium (PBTC). *Eur J Nucl Med Mol Imaging.* 2008;35:1651–1658.
121. Kruer MC, Kaplan AM, Etzl MM Jr, et al. The value of positron emission tomography and proliferation index in predicting progression in low-grade astrocytomas of childhood. *J Neurooncol.* 2009;95:239–245.
122. Zukotynski KA, Fahey FH, Kocak M, et al. Evaluation of ^{18}F-FDG PET and MRI associations in pediatric diffuse intrinsic brain stem glioma: a report from the Pediatric Brain Tumor Consortium. *J Nucl Med.* 2011;52:188–195.
123. Fulham MJ, Melisi JW, Nishimiya J, Dwyer AJ, Di Chiro G. Neuroimaging of juvenile pilocytic astrocytomas: an enigma. *Radiology.* 1993;189:221–225.
124. Sunada I, Tsuyuguchi N, Hara M, Ochi H. ^{18}F-FDG and ^{11}C-methionine PET in choroid plexus papilloma: report of three cases. *Radiat Med.* 2002;20:97–100.
125. Tsuyuguchi N, Matsuoka Y, Sunada I, Matsusaka Y, Haque M. Evaluation of pleomorphic xanthoastrocytoma by use of positron emission tomography with [18-F]-fluorodeoxyglucose and [^{11}C]-methionine tracers. *AJNR.* 2001;22:311–313.
126. Pirotte BJ, Lubansu A, Massager N, et al. Clinical interest of integrating positron emission tomography imaging in the workup of 55 children with incidentally diagnosed brain lesions. *J Neurosurg Pediatr.* 2010;5:479–485.
127. Phillips PC, Moeller JR, Sidtis JJ, et al. Abnormal cerebral glucose metabolism in long-term survivors of childhood acute lymphocytic leukemia. *Ann Neurol.* 1991;29:263–271.
128. Phillips PC, Dhawan V, Strother SC, et al. Reduced cerebral glucose metabolism and increased brain capillary permeability following high-dose methotrexate chemotherapy: a positron emission tomographic study. *Ann Neurol.* 1987;21:59–63.
129. Hipp SJ, Steffen-Smith EA, Patronas N, et al. Molecular imaging of pediatric brain tumors: comparison of tumor metabolism using ^{18}F-FDG-PET and MRSI. *J Neurooncol.* 2012;109:521–527.
130. Gilles R, Vogel WV, Gidding CE, Janssens GO, van der Vliet TM, Oyen WJ. ^{18}F-fluoro-L-thymidine-PET for the evaluation of primary brain tumours in children: a report of three cases. *Nucl Med Commun.* 2010;31:482–487.
131. Morana G, Piccardo A, Milanaccio C, et al. Value of ^{18}F-3,4-dihydroxyphenylalanine PET/MR image fusion in pediatric supratentorial infiltrative astrocytomas: a prospective pilot study. *J Nucl Med.* 2014;55:718–723.
132. Lopci E, Burnelli R, Ambrosini V, et al. ^{18}F-FDG PET in pediatric lymphomas: a comparison with conventional imaging. *Cancer Biother Radiopharm.* 2008;23:681–690.
133. Mody RJ, Bui C, Hutchinson RJ, et al. FDG PET imaging of childhood sarcomas. *Pediatr Blood Cancer.* 2010;54:222–227.
134. Cistaro A, Lopci E, Gastaldo L, Fania P, Brach Del Prever A, Fagioli F. The role of ^{18}F-FDG PET/CT in the metabolic characterization of lung nodules in pediatric patients with bone sarcoma. *Pediatr Blood Cancer.* 2012;59:1206–1210.

Downloaded from jnm.snmjournals.org by on March 5, 2020. For personal use only.

JNM The Journal of NUCLEAR MEDICINE

Value of ^{18}F-FDG PET and PET/CT for Evaluation of Pediatric Malignancies

Lebriz Uslu, Jessica Donig, Michael Link, Jarrett Rosenberg, Andrew Quon and Heike E. Daldrup-Link

J Nucl Med. 2015;56:274-286.
Published online: January 8, 2015.
Doi: 10.2967/jnumed.114.146290

This article and updated information are available at:
http://jnm.snmjournals.org/content/56/2/274

Information about reproducing figures, tables, or other portions of this article can be found online at:
http://jnm.snmjournals.org/site/misc/permission.xhtml

Information about subscriptions to JNM can be found at:
http://jnm.snmjournals.org/site/subscriptions/online.xhtml

The Journal of Nuclear Medicine is published monthly.
SNMMI | Society of Nuclear Medicine and Molecular Imaging
1850 Samuel Morse Drive, Reston, VA 20190.
(Print ISSN: 0161-5505, Online ISSN: 2159-662X)

© Copyright 2015 SNMMI; all rights reserved.

SNMMI SOCIETY OF NUCLEAR MEDICINE AND MOLECULAR IMAGING